

# FE-BI Analysis of a Leaky-Wave Antenna with Resistive Sheet Termination

Leo Kempel, Steve Schneider, Joshua Radcliffe, and Dan Janning, and Gary Thiele  
 Air Force Research Laboratory/ Sensors Directorate (AFRL/SNRR)  
 Wright-Patterson AFB, Dayton, OH 45433

**Abstract:** Printed leaky-wave antennas offer the potential for a low-profile, wide-bandwidth antenna element that can be arrayed if desired. Microstrip leaky-wave antennas rely on the suppression of the familiar  $\text{EH}_0$  mode and the propagation of the radiating  $\text{EH}_1$  mode. It is well-known that above a critical frequency, this leaky-wave will propagate with little attenuation and that the phase difference between the two radiating edges of the microstrip leads to radiation. However, due to the limits of installation area, such antennas must be terminated in a manner that reduces back reflection. If this is not done, a standing wave is established on the antenna limiting its utility as a leaky-wave antenna in terms of front-to-back ratio and bandwidth. In this paper, the hybrid finite element-boundary integral method is used to investigate an antenna termination scheme involving the use of resistive sheet extensions to the antenna. It will be shown that such a termination increases the front-to-back ratio and usable bandwidth of the antenna as compared to an antenna without such termination.

**Keywords:** Finite Element Method; Leaky-wave Antenna; Termination

## Introduction

Microstrip leaky-wave antennas offer the potential for a low-profile antenna with greater bandwidth than microstrip patch antennas. This is principally due to the fact that the radiation mechanism is attributed to a traveling-wave as compared to the standing-wave that is responsible for radiation by a microstrip patch antenna. The fundamental mode of a microstrip line, the so-called  $\text{EH}_0$  mode, is not a radiating mode (hence the popularity of microstrip transmission lines). The electric and magnetic fields for this mode are shown in Figure 1.

Rather, higher-order modes must be preferentially excited to realize a radiating traveling wave structure. The first higher-order mode, the  $\text{EH}_1$  mode, is one such radiating mode. This mode (shown in Figure 2) exhibits electric field odd symmetry about the axial centerline of the antenna as compared to the even symmetry of the  $\text{EH}_0$  mode.

One method for modeling the radiation from such an antenna is to consider an infinite cavity with perfect electrical conducting (PEC) surfaces representing the microstrip and the groundplane and perfect magnetic conducting (PMC) surfaces along the edges of the microstrip. The  $\text{EH}_0$  accordingly has two radiating edges, separated by the width of the antenna, with identical phase. Such a condition results in little radiation. However, the odd symmetry of the  $\text{EH}_1$  mode means that the phase of these two radiating edges are  $180^\circ$  apart and hence radiation occurs.

A common method for estimating the radiation bandwidth of an  $\text{EH}_1$ -mode antenna is based on a waveguide model [1-3]. The bandwidth of such an antenna is determined by the cut-off frequency for the  $\text{EH}_1$  mode and the frequency where the phase constant equals  $k_0$  (e.g. above this frequency, the bound mode propagates rather than the leaky-wave). This frequency range is given by

$$f_c = \frac{15}{w_{\text{eff}} \sqrt{\epsilon_r}} < f < \frac{f_c \sqrt{\epsilon_r}}{\sqrt{\epsilon_r - 1}} = \frac{15}{w_{\text{eff}} \sqrt{\epsilon_r - 1}} \quad (1)$$

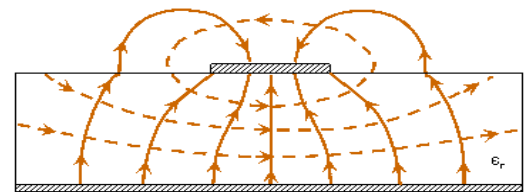


**Figure 1. Field diagram for the  $\text{EH}_0$  mode (E-field = solid, H-field = dashed).**

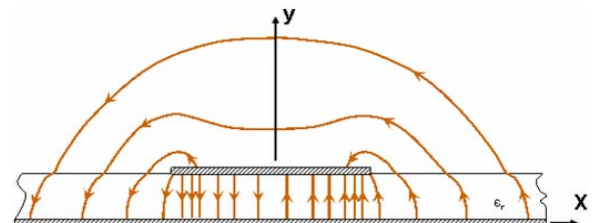


**Figure 2. Field diagram for the  $\text{EH}_1$  mode (E-field = solid, H-field = dashed).**

## Report Documentation Page

*Form Approved*  
*OMB No. 0704-0188*

Public reporting burden for the collection of information is estimated to average 1 hour per response, including the time for reviewing instructions, searching existing data sources, gathering and maintaining the data needed, and completing and reviewing the collection of information. Send comments regarding this burden estimate or any other aspect of this collection of information, including suggestions for reducing this burden, to Washington Headquarters Services, Directorate for Information Operations and Reports, 1215 Jefferson Davis Highway, Suite 1204, Arlington VA 22202-4302. Respondents should be aware that notwithstanding any other provision of law, no person shall be subject to a penalty for failing to comply with a collection of information if it does not display a currently valid OMB control number.

1. REPORT DATE <b>01 JAN 2005</b>	2. REPORT TYPE <b>N/A</b>	3. DATES COVERED <b>-</b>	
4. TITLE AND SUBTITLE <b>FE-BI Analysis of a Leaky-Wave Antenna with Resistive Sheet Termination</b>		5a. CONTRACT NUMBER	
		5b. GRANT NUMBER	
		5c. PROGRAM ELEMENT NUMBER	
6. AUTHOR(S)		5d. PROJECT NUMBER	
		5e. TASK NUMBER	
		5f. WORK UNIT NUMBER	
7. PERFORMING ORGANIZATION NAME(S) AND ADDRESS(ES) <b>Air Force Research Laboratory/ Sensors Directorate (AFRL/SNRR) Wright-Patterson AFB, Dayton, OH 45433</b>		8. PERFORMING ORGANIZATION REPORT NUMBER	
9. SPONSORING/MONITORING AGENCY NAME(S) AND ADDRESS(ES)		10. SPONSOR/MONITOR'S ACRONYM(S)	
		11. SPONSOR/MONITOR'S REPORT NUMBER(S)	
12. DISTRIBUTION/AVAILABILITY STATEMENT <b>Approved for public release, distribution unlimited</b>			
13. SUPPLEMENTARY NOTES <b>See also ADM001846, Applied Computational Electromagnetics Society 2005 Journal, Newsletter, and Conference., The original document contains color images.</b>			
14. ABSTRACT			
15. SUBJECT TERMS			
16. SECURITY CLASSIFICATION OF:			17. LIMITATION OF ABSTRACT
a. REPORT <b>unclassified</b>	b. ABSTRACT <b>unclassified</b>	c. THIS PAGE <b>unclassified</b>	<b>UU</b>
			18. NUMBER OF PAGES <b>4</b>
			19a. NAME OF RESPONSIBLE PERSON

where the zero-thickness effective width of the microstrip (in cm) is given by Wheeler [4-6]

$$w_{\text{eff}} = h \left\{ \frac{w}{h} + \frac{2}{\pi} \ln \left[ 2\pi e \left( \frac{w}{2h} + 0.92 \right) \right] \right\} \quad (2)$$

or alternatively, the effect of finite conductor thickness can be included [7]

$$\begin{aligned} \frac{w_{\text{eff}}}{h} &= \frac{w}{h} + \frac{1.25}{\pi} \frac{t}{h} \left[ 1 + \ln \left( \frac{4\pi w}{t} \right) \right] & \frac{w}{h} \leq \frac{1}{2\pi} \\ \frac{w_{\text{eff}}}{h} &= \frac{w}{h} + \frac{1.25}{\pi} \frac{t}{h} \left[ 1 + \ln \left( \frac{2h}{t} \right) \right] & \frac{w}{h} \geq \frac{1}{2\pi} \end{aligned} \quad (3)$$

In this work, since the finite element model will be assuming zero-thickness perfect electric conductors, the Wheeler formula (2) will be used.

Operation of the microstrip in the range of frequencies specified by (1) will allow the propagation of the  $\text{EH}_1$  leaky-wave mode; however, the fundamental  $\text{EH}_0$  will also propagate and depending on the feeding structure, this fundamental mode may dominate. One significant challenge in realizing a printed leaky-wave antenna is the suppression of the fundamental mode in preference to the desired  $\text{EH}_1$  mode. Various means of preferentially exciting the  $\text{EH}_1$  mode have been investigated (see for example [3] and the references contained within that manuscript). Another means of preferentially exciting the  $\text{EH}_1$  mode is to suppress the  $\text{EH}_0$  mode. This was accomplished using small slots in the microstrip structure near the feed region by Mentzel [8] and an asymmetric microstrip feed (including a quarter wave transformer to improve the match to a  $50\Omega$  port. An alternative method, utilizing a physical grounding structure along the length of the antenna, has recently been investigated by Thiele and his colleagues at the Air Force Research Laboratory [9]. The major advantage of such an antenna is the reduced width as compared to other leaky-wave microstrip antennas and the relatively simple feed structure. This present paper can be considered a companion paper to [10] in which the so-called half-width antenna is studied using a custom finite difference time domain (FDTD) code. In [10], a fictitious termination based on uniaxial perfectly matched layers (UPML) approach is used whereas in this present paper, a tapered resistive sheet is used to terminate the antenna and the hybrid finite element-boundary integral (FE-BI) method is used in the analysis. Before investigating this termination, it is useful to introduce the finite element method used in this analysis.

### Finite Element-Boundary Integral Model of the Half-width Antenna

The FE-BI method has been extensively reported upon in the literature and is extensively discussed in at least three popular text books on finite element methods for high frequency electromagnetics [11-13]. The FE-BI equations for a total electric field formulation may be written as

$$\begin{aligned} & \int_V \left[ \nabla \times \mathbf{W}_i \cdot \overline{\overline{\mu}}_r^{-1} \cdot \nabla \times \mathbf{W}_j \right] dV - k_0^2 \int_V \left[ \mathbf{W}_i \cdot \overline{\overline{\epsilon}}_r \cdot \mathbf{W}_j \right] dV + jk_0 \int_{S_R} \left[ \frac{(\hat{\mathbf{n}}_R \times \mathbf{W}_i) \cdot (\hat{\mathbf{n}}_R \times \mathbf{W}_j)}{R_e} \right] dS \\ & - k_0^2 \int_{S_a} \int_{S_a} \left[ \mathbf{W}_i \cdot \hat{\mathbf{z}} \times \overline{\overline{\mathbf{G}}}_{e2} \times \hat{\mathbf{z}} \cdot \mathbf{W}_j \right] dS' dS = \mathbf{f}_i^{\text{int}} + \mathbf{f}_i^{\text{ext}} \end{aligned} \quad (4)$$

where the first term is associated with the curl of the basis function (the magnetic field), the second term is associated with the basis function itself (the electric field), the third term is necessary to account for an resistive transition conditions if present, and the last term on the left-hand side is the boundary integral term (involving a second kind electric field dyadic Green's function). As shown, the placement of the material parameters  $(\overline{\overline{\epsilon}}_r, \overline{\overline{\mu}}_r)$  suggests that the basis functions  $(\mathbf{W}_j)$  and test functions  $(\mathbf{W}_i)$  should be chosen so that the dot products with the material tensors are accomplished readily. Accordingly, the right prism basis functions discussed in [14] are used herein. Additional information on implementing the FE-BI method is given in a recent Antennas and Propagation Magazine article [15].

The mesh for the half-width antenna that is the subject of this present paper is shown in Figure 3.

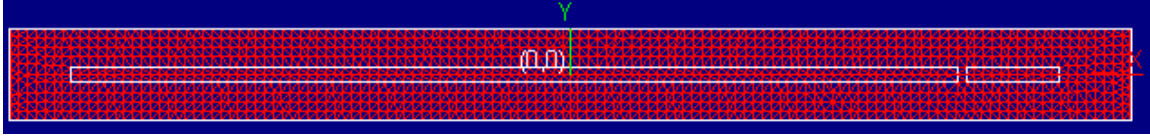


**Figure 3. Triangular surface mesh used to represent the half-width leaky-wave antenna.**

In this, the leaky wave antenna is shown as the long interior section. It is 19 cm long and 0.75 cm wide. There are  $1\Omega$  lumped loads placed every  $\lambda_0/10$  at 8 GHz (e.g. a pin every 1.5 cm) along the lower edge of the antenna. The smaller section, that is 3 cm long, is used to represent a resistive sheet (a.k.a. R-card) if such a load is present. If no load is present, a resistivity of  $10K\Omega/\text{sq.}$  is used. A set of  $1\Omega$  lumped loads are used to connect the R-card to the antenna. The board is assumed to be RT/Duroid 5870 ( $\epsilon_r = 2.33$ ) with a thickness of 31 mils (0.0787 cm). The cavity is chosen to minimize the aperture (and hence the number of boundary integral unknowns) due to limited memory on the available computers. This undoubtedly loads the antenna (and hence alters the results to some extent) although every effort has been made to minimize such loading.

### Results for the Half-width Antenna

The half-width antenna utilizes a physical electric conducting wall to suppress the fundamental  $\text{EH}_0$  mode. This is accomplished in the finite element model with periodic  $1\Omega$  resistors (in the actual antenna constructed in RASCAL at AFRL/SNRR, the wall is formed with conducting pins). The feed is a probe feed placed approximately half-way along the width of the half-width antenna (consistent with the placement of the co-planar microstrip feeds in [16]) and slightly inset. According to (1), the leaky-wave region of the antennas is given by  $6.55 \text{ GHz} \leq f \leq 8.67 \text{ GHz}$ . Below this range of frequency, the  $\text{EH}_1$  mode is in cut-off while above that range, the bound mode is dominant. In [10], the data generated from both the FDTD and transverse resonance models indicate that the attenuation of the propagating wave is quite small in the leaky-wave band and hence, a relatively short antenna (as is the one in this work) will have a significant backward traveling leaky-wave.

This study considers the impact of placing a tapered resistive sheet condition at the end of the microstrip antenna. The purpose of which it to reduce the level of a backward traveling wave and hence realize as close as possible the forward traveling wave results used to design such antennas. Note that this termination is physically realizable in comparison with the purely numerical termination. The choice of the taper is based upon an understanding of the leaky traveling wave. It is analogous to the traveling wave excited by  $\text{TE}_z$  incident field impinging on a PEC half-plane. Studies in the past have suggested the use of a gradual resistivity taper to a moderate end resistivity is a good means of softening the diffraction from such a half-plane. Hence, it is assumed that such a taper would also work well in reducing the reflection from a truncated leaky-wave microstrip line. For this work, a quadratic taper from  $1\Omega/\text{sq.}$  to  $50\Omega/\text{sq.}$  over a 3 cm length is used. This length was chosen to keep the over-all length of the antenna relatively small.

The VSWR (assuming a  $50\Omega$  feedline) is shown in Figure 4 comparing the VSWR of the unloaded and loaded antenna. As can be seen, the load has a significant effect on the VSWR for the leaky-wave region resulting in much less variation in VSWR w.r.t. frequency.

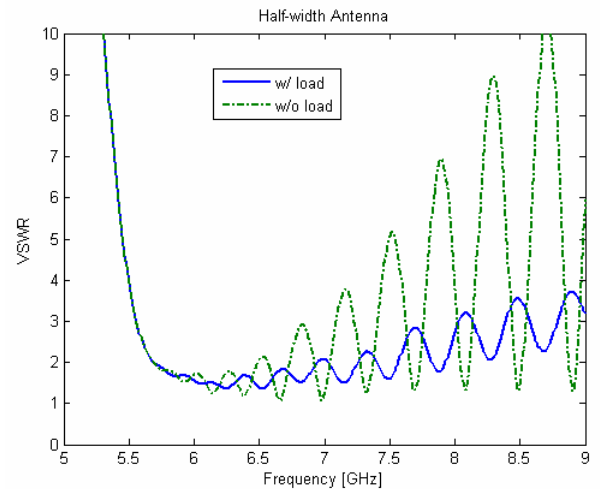


**Figure 4. Comparison of the VSWR for a loaded and unloaded half-width antenna.**

A comparison of the radiation pattern for the loaded and unloaded half-width antennas at 6.7 GHz is shown in Figure 5. The unloaded results are comparable to those presented in [10] in terms of the location of the peak radiation and in the front-to-back ratio. As can be seen, the front-to-back ratio is dramatically improved (on the order of 10 dB) through the use of the resistive sheet termination.

### Conclusions

In this paper, the hybrid finite element-boundary integral method was used to investigate the properties of a leaky-wave antenna. The antenna under study was the half-width antenna recently introduced by Radcliffe *et al.* [9]. In this, a physical structure (realized via periodic shorting pins) is used to suppress the fundamental -- even-- mode. Probe feeding was used in the model since this antenna does not require a sophisticated feed structure as was needed in [16] to suppress the fundamental mode. In particular, the behavior of the antenna in terms of VSWR, radiation power gain, and normal electric fields was investigated for two cases: an unloaded half-width antenna and a loaded half-width antenna. The load was a short quadratically tapered resistive sheet attached co-planar to the end of the microstrip line.

Use of the resistive load dramatically reduces the backward traveling leaky-wave and hence improves the front-to-back ratio and 2:1 VSWR bandwidth. This termination has not been optimized. It is noted that a longer termination will yield better results; however, at the obvious expense of a larger aperture.

### References

1. C.S. Lee, V. Nalbandian, and F. Scherwing, "Planar dual-band microstrip antenna," *IEEE Trans. Antenna. Propagat.*, 43, pp. 892-895, Aug. 1995.
2. C.S. Lee and V. Nalbandian, "Planar leaky-wave microstrip antenna," *Proc. IEEE AP-S Int. Symp. Dig.*, pp. 1126-1129, 1997.
3. W. Hong, T-L Chen, C-Y Chang, J-W Sheen, and Y-D Lin, "Broadband tapered microstrip leaky-wave antenna," *IEEE Trans. Antennas Propagat.*, 51, pp. 1922-1928, Aug. 2003.
4. H.A. Wheeler, "Transmission line properties of parallel wide strips by conformal mapping approximation," *IEEE Trans. Microwave Theory Tech.*, 12, pp. 280-289, 1964.
5. H.A. Wheeler, "Transmission line properties of parallel strips separated by a dielectric sheet," *IEEE Trans. Microwave Theory Tech.*, 13, pp. 172-185, 1965.
6. I. Wolff, "The waveguide model for the analysis of microstrip discontinuities," Chpt. 7 in Numerical Techniques for Microwave and Millimeter-wave Passive Structures, T. Itoh (Ed.), Wiley Interscience: New York, 1989.
7. I.J. Bahl and R. Garg, "Simple and accurate formulas for a microstrip with finite strip thickness," *IEEE Proc.*, 65, pp. 1611-1612, Nov. 1977.
8. W. Menzel, "A New Traveling-Wave Antenna in Microstrip", *Archiv fur Elektronik und Ubertragungstechnik (AEU)*, Band 33, Heft 4:137-140, April 1979.
9. J.S. Radcliffe, G.A. Thiele, and G. Zelinski, "A microstrip leaky wave antenna and its properties, 26<sup>th</sup> Antenna Measurement Tech. Assoc. Meeting, St. Mountain, GA, Oct. 2004.
10. G.M. Zelinski, M.L. Hastriter, M.J. Havrilla, J.S. Radcliffe, A.J. Terzuoli, and G.A. Thiele, "FDTD analysis of a new leaky traveling wave antenna," submitted to the 2005 *IEEE/ACES Intl. Conf.*, Honolulu, Hawaii, Apr. 2005.
11. J.L. Volakis, A. Chatterjee, and L.C. Kempel, *Finite Element Methods for Electromagnetics*, IEEE Press: Piscataway, N.J., 1998.
12. M. Salazar-Palma, T. Sarkar, L-E Garcia-Castillo, T. Roy, and A. Djordjevic, *Iterative and Self-Adaptive Finite-Elements in Electromagnetic Modeling*, Artech House: Norwood, MA, 1998.
13. J-M Jin, *The Finite Element Method in Electromagnetics*, 2<sup>nd</sup> Ed., Wiley: New York, 2002.
14. L.C. Kempel, "Implementation of Various Hybrid Finite Element-Boundary Integral Methods: Bricks, Prisms, and Tets," 1999 *ACES Meeting*, Monterey, CA, pp. 242-249, 1999.
15. A. Awadhiya, P. Barba, and L. Kempel, "Finite-element method programming made easy???", *IEEE Antennas and Propagation Magazine*, 45, pp. 73-79, Aug. 2003.
16. Y-D Lin, J-W Sheen, and C-K. C. Tzuang, "Analysis and design of feeding structures for microstrip leaky wave antennas," *IEEE Trans. Microwave Theory Tech.*, 44, pp. 1540-1547, Sept. 1996.

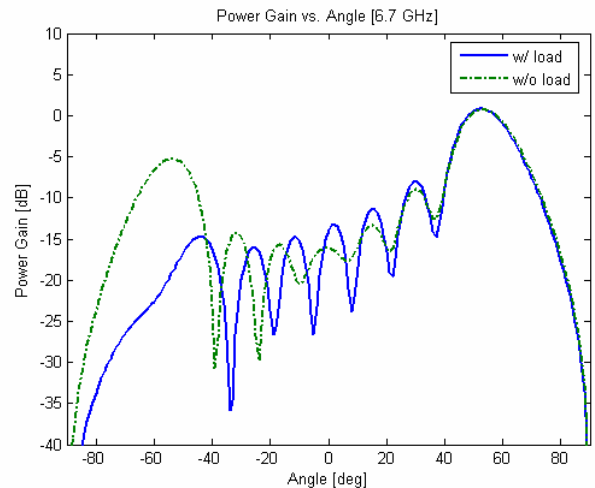


**Figure 5. Comparison of power gain patterns for the loaded and unloaded half-width antennas at 6.7 GHz.**